Spatiotemporal soliton propagation in saturating nonlinear optical media

V. Skarka
Laboratoire POMA, EP 130 CNRS, Université d'Angers, 2, boulevard Lavoisier, 49045 Angers, Cedex 1, France

V. I. Berezhiani
International Center for Theoretical Physics, 34100 Trieste, Italy
and Institute of Physics, The Georgian Academy of Sciences, Tbilisi 380077, Georgia

R. Miklaszewski
Institute of Plasma Physics and Laser Microfusion, Hery street 23, 00-908 Warsaw, P.O. Box 49, Poland
(Received 7 October 1996)

The simultaneous balance of nonlinear spatial self-focusing with diffraction and the compensation of dispersion with nonlinear temporal self-focusing, in a saturating nonlinear medium, give stable spatiotemporal solitons, or ''light bullets.'' An analytical approach for arbitrary saturating nonlinearity is established in order to investigate the dynamics of such light bullets. This approach is applied to nonlinear materials with negative fourth-order optical index. The analytically predicted exceptional robustness of light bullets that can be generated in a large range of parameters is confirmed by numerical simulations. [S1063-651X(97)01207-5]

PACS number(s): 42.65.Tg

I. INTRODUCTION

Optical solitons may soon become the principal carrier in telecommunication because, as self-confined structures, they propagate long distances without changing shape [1]. Long-distance information transmission is realized in optical fibers using temporal solitons created by the balance of induced phase chirp due to dispersion with the nonlinearly induced self-phase modulation. The binary information once brought by temporal solitons has to be retreated in all-optical systems, where in principle the solitons have to satisfy the requirement of being self-guided in bulk media [2,3]. Therefore, there is a growing interest for spatiotemporal solitons, characterized by a balance of diffraction and dispersion with respectively nonlinear spatial and temporal self-focusing. The dynamics of such localized structures is governed by a $(3+1)$-dimensional nonlinear Schrödinger equation (NSE) containing one propagation dimension and three ''transverse'' dimensions [3]. The equation treats time and space dimensions identically.

The materials used in optical systems are usually of Kerr type [4]. Consequently, the dynamics of the electromagnetic (EM) pulses is described by a NSE with cubic nonlinearity (CNSE). It is well known that only solutions of $(1+1)$-dimensional CNSE are stable [5]. These exact analytical solutions obtained by the inverse-scattering method correspond to one-dimensional temporal or spatial solitons. However, NSE with saturating nonlinearities have in some circumstances stable soliton solutions even for two or three transverse dimensions [6]. Such solitons completely localized in three space and one time dimensions are called ''light bullets'' [3]. The light bullets are of both fundamental and technological interest, since they satisfy the best requirements for digital optical logic [2]. Taking into account that materials currently used in optical systems exhibit weak saturation effects, there is an increasing interest in those materials that can sustain stable propagation of solitons limiting the growth of nonlinear index. The inclusion of the third term in the power series expansion of the nonlinear optical index, $\delta n(I)$ with respect to intensity I,

$$n = n_0 + \delta n(I) = n_0 + n_2 I + n_4 I^2 \tag{1}$$

(n_0 is linear index) leads to flattening at higher intensities, under the condition that the fourth-order index is negative. Recent measurements of organic nonlinear materials show that such a requirement can be fulfilled, for instance, for polydiacetylene *para*-toluene sulfonate (PTS) [7]. This material is promising since it should yield solitons at low power [8].

However, for higher dimensional NSE there are no exact analytical methods to derive nonstationary solutions. One often has to rely on computer simulations in order to investigate the solutions of such equations.

General dynamical properties of nonstationary solutions are rather complex, making analytical approximations highly desirable. To describe the dynamics of localized solutions of NSE, various approximation schemes such as the paraxial ray theory [9], the moment theory [10], and the variational approach [11], have been developed.

In the present work we will study the dynamics of the light bullets in saturating media combining the variational method with numerical simulations. A general analytical approach for every transverse dimension, $D=1,2,3$, and an arbitrary saturating nonlinearity will be given in Sec. II. This general approach will be applied to nonlinear materials with negative fourth-order optical index, in order to study the conditions under which the propagation of light bullets is stable (Sec. III). Using analytical results as a guide for numerical simulations, the studies of exact soliton dynamics are carried on in Sec. IV.

II. GENERAL APPROACH BASED ON THE VARIATIONAL PRINCIPLE

The interaction of a finite amplitude optical pulse with a nonlinear bulk medium gives rise to a slowly varying optical

field envelope $\mathcal{E}$ corresponding to a quasi-monochromatic electric field with carrying frequency ω. The equation for pulse propagation along the z axis is

$$2ik\left(\frac{\partial\mathcal{E}}{\partial z}+\frac{1}{v_g}\frac{\partial\mathcal{E}}{\partial t}\right)+\Delta_\perp\mathcal{E}-k\frac{d^2k}{d\omega^2}\frac{\partial^2\mathcal{E}}{\partial t^2}+2k^2\frac{\delta n(|\mathcal{E}|^2)}{n_0}\mathcal{E}=0, \tag{2}$$

where v_g is the group velocity of the pulse, $k=n_0\omega/c$ is the wave vector, and $\Delta_\perp=(\partial^2/\partial x^2+\partial^2/\partial y^2)$ is the two-dimensional (2D) Laplacian describing beam diffraction. In what follows we assume that the optical medium exhibits an anomalous group velocity dispersion $d^2k/d\omega^2<0$.

Introducing a ''moving'' coordinate $\tau=t-z/v_g$, and making a self-evident renormalization of the variables, Eq. (2) can be rewritten in dimensionless form as

$$i\frac{\partial E}{\partial z}+\frac{\partial^2E}{\partial\tau^2}+\Delta_\perp E+f(|E|^2)E=0, \tag{3}$$

where E is the slowly varying amplitude of the electric field $\mathcal{E}$ properly redefined corresponding to the nonlinearity under consideration. The function $f(u)$ is generally complex valued and it obeys the requirement $f(u)u|_{u\to0}=0$. Equation (3) describes spatial and temporal self-focusing of electromagnetic pulse propagating under the combined effects of diffraction and dispersion.

Let us look for a ''spherical'' symmetric distribution of the fields. Notice that the comoving coordinate (τ) can be treated on an equal footing as a spatial coordinate. In terms of the radial variable $r=(x^2+y^2+\tau^2)^{1/2}$, Eq. (3) can be rewritten as

$$i\frac{\partial E}{\partial z}+\frac{1}{r^{D-1}}\frac{\partial}{\partial r}\left(r^{D-1}\frac{\partial E}{\partial r}\right)+f(|E|^2)E=0, \tag{4}$$

where the transverse dimension D can be 1, 2, or 3.

The Lagrangian density corresponding to Eq. (4) is

$$L=-r^{D-1}\left|\frac{\partial E}{\partial r}\right|^2+\frac{i}{2}r^{D-1}\left(E^*\frac{\partial E}{\partial z}-E\frac{\partial E^*}{\partial z}\right)+r^{D-1}F(|E|^2), \tag{5}$$

where the asterisk denotes complex conjugate and

$$F(u)=\int_0^u f(u')du'. \tag{6}$$

An appropriate variation of Lagrangian, $\delta L/\delta E^*=0$, yields Eq. (4) as the Euler-Lagrange equation.

It is easy to prove by direct computation [or using Noether's theorem for the Lagrangian (5)] that Eq. (4) conserves the following integrals of motion: the ''photon number''

$$\mathcal{N}=\int_0^\infty drr^{D-1}|E|^2, \tag{7}$$

and the Hamiltonian

$$\mathcal{H}=\int_0^\infty drr^{D-1}\left[\left|\frac{\partial E}{\partial r}\right|^2-F(|E|^2)\right]. \tag{8}$$

As we mentioned in the Introduction, to describe analytically the dynamics of localized solutions of Eq. (4) two methods seem to be appropriate: the moment theory and the variational approach. The moment theory is based on the integrals of motion [Eqs. (7) and (8)] and on the equation for the mean square radius of the beam (i.e., on the so-called ''virial theorem'' [6]).

In this paper we use the variational approach that, being equivalent to the moment method, gives a better and simpler treatment of the problem. In the optimization procedure, the first variation of the corresponding functional must vanish on a set of suitably chosen trial functions. As trial functions, we will use Gaussian shaped pulses. Such a choice greatly simplifies computations. Thus, we assume that the evolution of the pulse can be characterized by the trial function

$$E=A(z)\exp\left[-\frac{r^2}{2a(z)^2}+ir^2b(z)+i\phi(z)\right], \tag{9}$$

with amplitude A, beam ''radius'' a, wave front curvature b, and phase ϕ as unknown functions of propagation coordinate z, which will be furthermore used in order to make the variational functional an extremum. The Lagrangian can be expressed in terms of these parameters of the trial function,

$$L=-r^{D+1}|E|^2\left(\frac{1}{a^4}+4b^2\right)-|E|^2r^{D+1}\frac{db}{dz}-|E|^2r^{D-1}\frac{d\phi}{dz}+r^{D-1}F(|E|^2). \tag{10}$$

To make the time dependent problem tractable, an averaging over radial coordinate is helpful. Such an averaging yields

$$\langle L\rangle=\int_0^\infty drL=-\left(\frac{1}{a^4}+4b^2+\frac{db}{dz}\right)A^2a^{D+2}D-2\frac{d\phi}{dz}A^2a^D+a^DK(A^2), \tag{11}$$

with

$$K(u)=\frac{4}{\Gamma[D/2]}\int_0^\infty dpp^{D-1}F(ue^{-p^2}), \tag{12}$$

where Γ is Gamma function.

The set of Euler-Lagrange equations can be derived under the condition that the variation with respect to each of unknown functions should be zero, $\delta\langle L\rangle/\delta Q=0$, where $Q=(A^2,a,b,\phi)$.

After some algebra, we get the following set of ordinary differential equations:

$$A^2a^D=A_0^2a_0^D, \tag{13}$$

$$\frac{d^2a}{dz^2}=\frac{4}{a^3}-\frac{2}{a}\left[K'(A^2)-\frac{K(A^2)}{A^2}\right], \tag{14}$$

$$\frac{d\phi}{dz}=-\frac{D}{a^2}+\frac{1}{4}\left[(D+2)K'(A^2)-D\frac{K(A^2)}{A^2}\right], \tag{15}$$

$$b=\frac{1}{4a}\frac{da}{dz}, \tag{16}$$

to be solved for the four functions A, a, b, and ϕ. Here A_0 and a_0 are, respectively, the initial amplitude and the initial ''radius'' of the EM beam at $z=0$.

Equation (13) is simply a statement of the fact that during the EM pulse evolution its ''energy,'' $N=A^2a^D$ is conserved. Using Eq. (13), the integration of Eq. (14) gives

$$\frac{1}{2}\left(\frac{da}{dz}\right)^2+V(a)=H=V(a_0), \tag{17}$$

where

$$V(a)=\frac{2}{a^2}-\frac{2a^D}{Da_0^DA_0^2}K\left(\frac{A_0^2a_0^D}{a^D}\right) \tag{18}$$

plays the role of an effective potential for the evolution of the radius a. We have assumed that the initial beam has a plane front (or zero curvature) $[da/dz|_{z=0}=0=b(0)]$. Notice that the constants of integration N and H normalized by the factor $\Gamma[D/2]/2$ actually represent, respectively, ''photon number'' $\mathcal{N}$ and Hamiltonian $\mathcal{H}$ obtained from Eqs. (7), (8), and (9). In what follows, N denotes the beam energy and H the Hamiltonian.

Using the analogy with a particle in a potential well, we can acquire a deeper physical understanding of light beam dynamics. Choosing the initial beam radius a_0 equal to the equilibrium radius a_e, a stationary solution of Eq. (14) is obtained if $\partial V/\partial a|_{a=a_e}=0$. Note that $-\partial V/\partial a$ is equal to the right-hand side of Eq. (14). The equilibrium radius of the beam is readily found to be

$$a_e^2=2\left[K'(A_0^2)-\frac{K(A_0^2)}{A_0^2}\right]^{-1}. \tag{19}$$

The stability of the equilibrium solution $a_0=a_e$ can be checked by studying the behavior of small amplitude disturbances around this equilibrium. Linearizing Eq. (14) around the equilibrium solution ($a=a_e+\delta a$, $a_e\gg\delta a$) we get

$$\frac{d^2}{dz^2}\delta a+\Omega^2\delta a=0, \tag{20}$$

where

$$\Omega^2=\left.\frac{\partial^2V}{\partial a^2}\right|_{a=a_0}=\frac{1}{a_0^2}\left[\frac{4+2D}{a_0^2}-DA_0^2K''(A_0^2)\right]. \tag{21}$$

If Ω^2 is positive, the equilibrium solution is stable. The condition $\Omega^2>0$ can also be written as $dN_e/dA_0>0$ where N_e is the energy of the pulse corresponding to the equilibrium. Notice that this condition is equivalent to the well-known stability criterion of Vakhitov and Kolokolov derived using the moment theory [6].

In deriving the system of equations (13)–(21) we did not use an explicit form for the functions $f(|A|^2)$; thus the established formalism can be applied to the NSE with an arbitrary nonlinear term.

For the saturating nonlinearity $V(a)|_{a\to0}\to\infty$, which means that the beam radius is bounded from below. Consequently, the so-called collapse does not occur. The beam is either trapped and forms an oscillating waveguide or diffracts monotonically. For the oscillating beam radius there are two distinct modes of behavior (see, for instance, Fig. 4). (i) When $a_0>a_e$, the slope of the potential is positive, $\partial V/\partial a|_{a=a_e}>0$ and the beam radius initially contracts until it reaches the smallest value given by the turning point $a_-(<a_e)$. (ii) If $a_0<a_e$ the slope is negative, $\partial V/\partial a|_{a=a_e}<0$, and the beam radius initially increases. Further evolution depends on the value of constant Hamiltonian H [see Eq. (17)]. If $H<0$, the beam never diffracts and enters the self-trapped regime. This agrees with the general criterion in the moment approach established by Zakharov *et al.* [12], that if the Hamiltonian $\mathcal{H}$ is negative there is no diffraction since the maximum value of the field intensity has a z-independent lower bound $|E|^2_{\max}>|\mathcal{H}|/\mathcal{N}$.

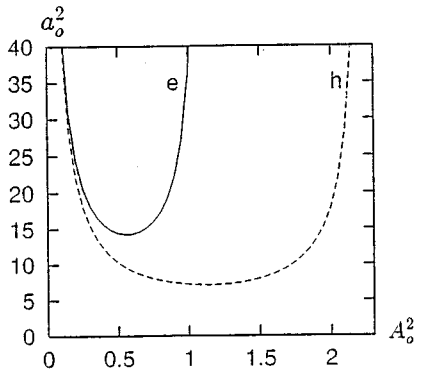

FIG. 1. Equilibrium curve e (solid line) and zero Hamiltonian curve h (dashed line) for the 2D case.

III. SATURATING NONLINEARITY WITH NEGATIVE FOURTH-ORDER OPTICAL INDEX

In nonlinear optics several types of saturating nonlinearities are discussed [11]. As we mentioned in the Introduction a large nonresonant nonlinearity has been found in polydiacetylene *para*-toluene sulfonate [7].

In the subsequent analysis we will consider a nonlinear term of the following form:

$$f(|E|^2)=|E|^2-|E|^4. \tag{22}$$

This kind of nonlinearity, but assuming that $|E|^2\ll1$, has been considered in several previous publications [12,13]. For PTS the second term in the right-hand side of Eq. (22) can be of the same order as the first one [8].

In order to study the conditions under which solitons can propagate in such a material, we will apply the established general formalism to the saturating nonlinearity given by Eq. (22). For the function K [see Eq. (12)] one gets

$$K(A^2)=\alpha A^4-\beta A^6, \tag{23}$$

where $\alpha=2^{(-D/2)}$ and $\beta=2\times3^{(-D/2-1)}$. The equilibrium radius of the beam, obtained from Eq. (19),

$$a_e^2=\frac{2}{\alpha A_0^2-2\beta A_0^4}, \tag{24}$$

is plotted in the (a_0^2,A_0^2) plane (see curve e in Figs. 1 and 2).

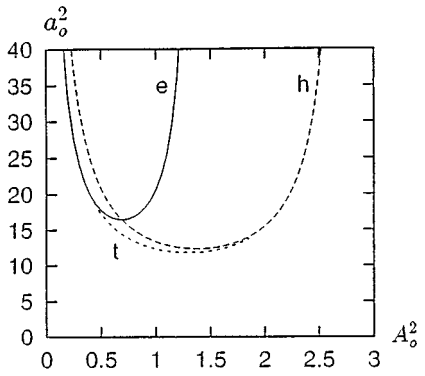

FIG. 2. Equilibrium curve e (solid line), zero Hamiltonian curve h (dashed line), and trapping curve t (dotted line) for the 3D case.

In the region that lies above this curve the beam radius oscillates with initial focusing.

The equilibrium solution is stable ($\Omega^2>0$), i.e., it is a soliton, if the condition

$$A_0^2>\frac{\alpha}{4\beta}\frac{D-2}{D-1} \tag{25}$$

is satisfied. For 1D and 2D cases the equilibrium solution is stable for arbitrary beam amplitude, since the inequality (25) is always satisfied. For 3D case, the solution is stable only if $A_0>(\alpha/8\beta)^{1/2}(\approx 0.58)$. Thus the small amplitude ($A_0<0.58$) equilibrium solutions are unstable.

As mentioned above, if the Hamiltonian is negative ($H<0$) then the beam always forms an oscillating waveguide. From Eqs. (17) and (18), one obtains the beam radius corresponding to the zero Hamiltonian

$$a_H^2=\frac{D}{\alpha A_0^2-\beta A_0^4}, \tag{26}$$

which is plotted as curve h in Figs. 1 and 2. It can be seen that if $a_0^2>a_H^2$, for given A_0^2, then $H<0$.

In 1D and 2D cases the inequality $a_e>a_H$ always holds. Analyses of Eq. (18) shows that in 1D and 2D cases, the beam always diffracts monotonously if $a_0<a_H$ (i.e., if $H>0$). Notice that for the 1D case the plot has the same structure as in the 2D case, so the 1D case is omitted from Fig. 1.

The particularity of the 3D case is that $a_e>a_H$ only if the initial amplitude is sufficiently big, $A_0^2>(\alpha/4\beta)$. The self-trapping of the beam is, however, possible even for a positive Hamiltonian. Indeed, if $A_0^2<\alpha/4\beta$ then $a_e<a_H$ and, consequently, the equilibrium solution corresponding to the soliton appears in the range of $H>0$ also. In what follows we consider only the 3D case.

In order to get better insight into the dynamical behavior of the pulse, we plot in Fig. 3 the conserved energy N as a function of the squared amplitude of the pulse A^2. The solid line corresponds to the equilibrium and the dashed one to the zero Hamiltonian. The light bullet is trapped in an oscillating waveguide provided its energy N is bigger than the critical value given by $N_c=35.3$. Note that the equilibrium is stable,

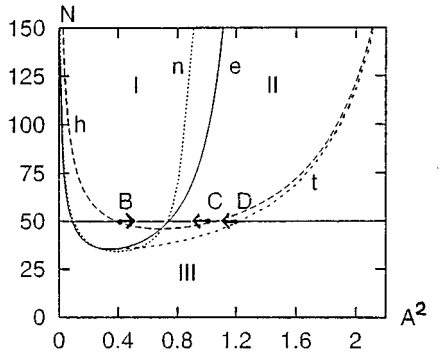

FIG. 3. Energy N as a function of A^2 for the 3D case. Equilibrium curve e (solid line) together with the numerically obtained equilibrium line n (dotted line), curve h, and trapping curve t (both dashed). I: focusing region, II: defocusing region; and III: diffraction region.

$dN/dA^2>0$ if $A^2>0.34$. Thus for every given $N>N_c$ we have two equilibria, however, only the stable one plays the role of an attractor for each of the points initially located in the regions (I) and (II). This can be easily seen from Fig. 4, analyzing the shape of potential V as a function of radius a and energy N,

$$V(a,N)=\frac{2}{a^2}-\frac{2\alpha N}{3a^3}+\frac{2\beta N^2}{3a^6} \tag{27}$$

obtained from Eqs. (13), (17), and (18).

The front lines (Fig. 4) correspond to the sections with constant energy N smaller than the critical one N_c and the beam diffracts monotonously.

In the supercritical case, $N>N_c$, the potential has two extrema, minimum and maximum. Therefore, depending on $H=V(a_0,N)$ the beam will be either trapped or will diffract. The beam with initial radius corresponding to the point lying on the potential curve somewhere below the maximum will be always trapped, creating a light bullet with oscillating radius. Starting from the negative slope of the potential, the beam will first diffract (region II in Fig. 3); being on the positive slope, it will first focus (region I). Only if the initial

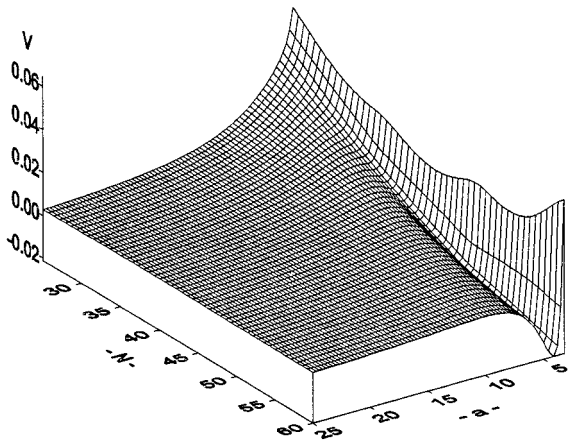

FIG. 4. Diffraction for subcritical energies $N<N_c$ and self-guiding in the supercritical case.

conditions are chosen to be on the stable part of curve *e*, the light bullet will have a constant (equilibrium) radius, since it is already on the bottom of the potential well. However, if the initial radius is so small that it corresponds to a potential larger than its extremum (maximum), the beam can diffract forever. For $N=N_c$ the potential curve is broken at the point where minimum and maximum coincide, which corresponds to the touching point between stable and unstable equilibrium on curve *e* of Fig. 3.

The trapping line *t* in Figs. 2 and 3 asymptotically approaches curve *h* of the zero Hamiltonian for large amplitude. Above the trapping line (regions I and II in Fig. 3) the light bullets can be created even for a positive Hamiltonian. Below this line (region III) monotonic diffraction occurs.

Dynamics of pulsating light bullets clearly follows from Figs. 3 and 4. Using the variational method it can be predicted that for a constant energy *N* (the horizontal line in Fig. 3) all beams initially in region *I*, or equivalently on the positive slope, will form light bullets pulsating around its equilibrium radius with initial focusing until the turning point in region II, which can be exactly computed knowing initial conditions. For initial points in region III, the beam will always diffract even though it crosses the equilibrium line. For instance, being initially on the right of the trapping line in Fig. 3, the diffracting beam amplitude will decrease from its maximum value, crossing region II, overshooting the stable equilibrium as well as the unstable one.

In the preceding analysis, we applied a variational approach involving a Gaussian trial function. It is also possible to use trial functions of different kinds, for instance the super Gaussian one, which may fit the equilibrium profile better than the Gaussian. However, the approach we are using for nonsteady propagation provides in a good approximation explicit analytical expressions for beam evolution. The main conclusion that follows from the present analyses is the existence of the stable equilibrium, which plays the role of an attractor, provided $N>N_c$. For a given energy *N*, the beam will be self-trapped in a wide range of parameters: not only in the domain of the negative Hamiltonian but also in a part of the region where $H>0$. Such a self-trapped beam generates a light bullet that will pulsate near the stable equilibrium.

IV. NUMERICAL SIMULATION OF THE LIGHT BULLET BEHAVIOR

The main limitation of various approaches, such as the paraxial, momentum, or variational approaches, is that they are valid only in the aberrationless approximation; i.e., they are unable to account for structural changes in the beam shape. It is also obvious that in the case of big saturating nonlinearities the fundamental, i.e., ground state, soliton profile can be quite different from the Gaussian one. Such aspects of the beam dynamics are better delineated by numerical simulations, although the guidelines for simulation are still provided by approximative analytical approaches.

In this section we present the results of numerical simulations of Eq. (4) for initially Gaussian-shaped beam in the 3D case. The obtained simulation data can be qualitatively understood and interpreted, using the analytical results of the previous section.

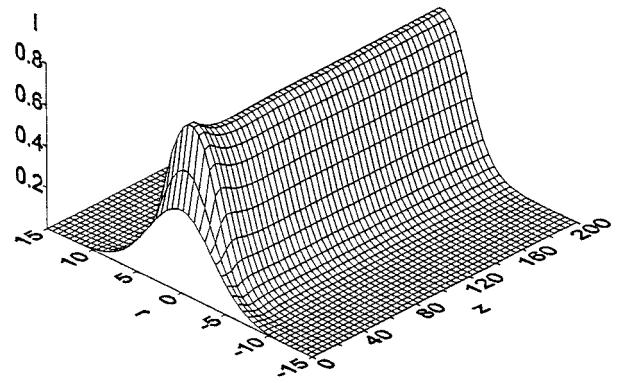

FIG. 5. Generation of a stable light bullet with initial focusing for energy $N=50$ and initial intensity $A_0^2=0.4$.

The numerical simulations give $N_c=34.04$ for the beam trapping critical energy. This is the minimum of the dotted line *n* in Fig. 3, which corresponds to the exact numerical solution of Eq. (4) for the ground state soliton. Such a soliton with maximal amplitude A_m is stable if $A_m^2>0.41$. These results agree with those of Ref. [2]. For a large amplitude soliton, the results of the variational approach (based on the Gaussian trial function) deviate markedly from exact numerical solutions.

Numerical simulations show that if an initial profile of the beam is close to the stable equilibrium one (the exact numerical solution), the beam quickly attains the profile of ground state soliton and propagates for a long distance without distortion of its shape. Even if the initial beam is in a domain of parameters corresponding to the profile quite far from the equilibrium one, this beam will, however, either focus or defocus to the ground state equilibrium exhibiting damped oscillations around it. The pulsations are damped due to the appearance of the radiation spectrum. This is shown in Figs. 5–8, where the field intensity ($I=|E|^2$) distribution is plotted versus radius *r* and the propagating coordinate *z*, for the initially Gaussian shaped beam $|E(r,0)|=A_0\exp[-r^2/2a_0^2]$. In all these cases the parameters of the beam (i.e., A_0 and a_0) are chosen to give the same energy $N=A_0^2a_0^3=50$ (the horizontal line in Fig. 3). Although the initial amplitudes of the beam (points *B*, *C*, and *D* in Fig. 3) are quite different from the amplitude of the corresponding equilibrium soliton, in all these cases light bullets appear, exhibiting damped pulsations near the equilibrium. Starting from the initial point *B* (in domain I of Fig. 3), the amplitude first increases in Fig. 5, which corresponds to an initial focusing as predicted analytically. Then the equilibrium amplitude is a bit overshot in order to be reached immediately after. Other tested initial points *C* and *D* belong to the domain II with initial defocusing. Accordingly, a sudden decrease of amplitude in Figs. 6 and 7 is followed by a damped pulsation until stable equilibrium is reached. Either the initial focusing or defocusing before reaching the equilibrium can be better seen in Fig. 9, where the field $|E(0,z)|$ is drawn for different initial points *B*, *C*, and *D*.

Initial conditions *B* and *C* correspond to the negative Hamiltonian. This is in agreement with Zakharov's criterion [12] that the beam cannot undergo permanent diffraction corresponding to boundless decreasing of field intensity. This

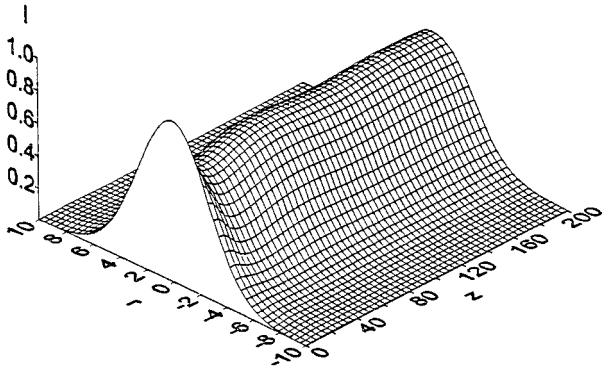

FIG. 6. Light-bullet generation. Initial defocusing for energy $N=50$ and initial intensity $A_0^2=1$.

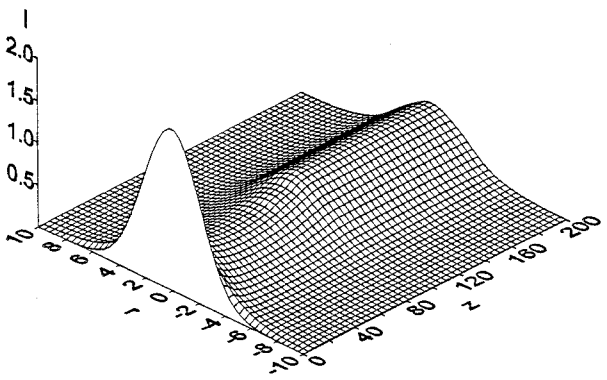

FIG. 8. Formation of a light bullet out of regions predicted by the analytical approach. Initial intensity is $A_0^2=1.9$ for $N=50$.

means that, provided the filamentation does not occur, the beam will be trapped, creating oscillating field structure. Note that the possibility of collapse is excluded for saturating nonlinearities, since the beam is bounded from below as established in Sec. II.

A peculiarity of the 3D case is that the beam enters in the self-trapped regime even when $\mathcal{H}>0$. This fact is clearly demonstrated in the previous section using the variational approach and it is also considered numerically in Fig. 7.

The simulations show that for $N=50$ the large amplitude beam enters in the self-trapped regime provided $A_0^2 \leqslant 1.9$ (see Fig. 8). This amplitude, separating the self-trapping domain from the diffracting one, is bigger than predicted by the variational approach, because of its inability to take into account the structural changes of beam shape. If $A_0^2>1.9$, the beam will diffract completely.

It can be concluded that the numerical simulations confirm exceptional robustness of light bullets, which can be generated in a large range of parameters, even far from stable equilibrium, as predicted by our analytical approach.

V. DISCUSSION AND CONCLUSIONS

The results obtained in previous sections may be applied to the materials exhibiting saturating nonlinearity with negative fourth-order optical index, like PTS for instance. Using laser wavelength $\lambda=1.6\ \mu$m, the measured values of second and fourth-order optical index for PTS are, respectively, $n_2=2.2\times10^{-3}$ cm^2/GW and $n_4=-0.8\times10^{-3}$ cm^4/GW^2 [7]. This material is promising since it has the largest nonresonant nonlinearities. Therefore, due to low power requirement, PTS can be a good candidate for all-optical switching and may be used in telecommunications [8]. Recently it was shown experimentally that solitons with two transverse spatial dimensions can be generated in bulk PTS at 1.6 μm [14]. However, the temporal confinement related to the duration of pulses has not been investigated. Such a confinement involves anomalous group velocity dispersion. Unfortunately the PTS exhibits the normal group velocity dispersion, as majority of transparent materials [15]. Using an appropriate technique (for instance, grating) the frequency distribution in the pulse may be inverted creating an effective anomalous dispersion necessary for light-bullet propagation [2]. However, this inversion will alter Eq. (2). Nevertheless, in order to give some rough estimations of light-bullet size and required energy we will use the value for optical indices of a hypothetical inverted PTS supposing that the corrections to the equations due to this inversion are small. The anoma-

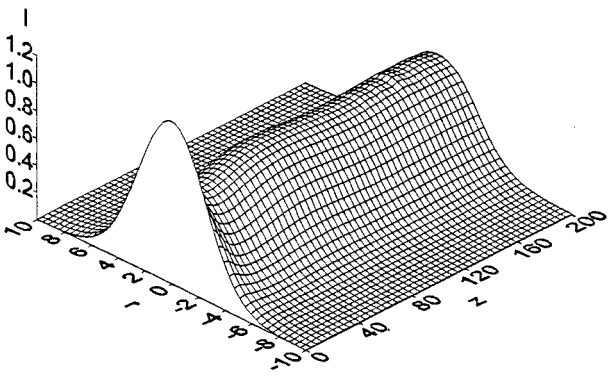

FIG. 7. Generation of a light bullet with initial defocusing in the case of positive Hamiltonian for energy $N=50$ and initial intensity $A_0^2=1.2$.

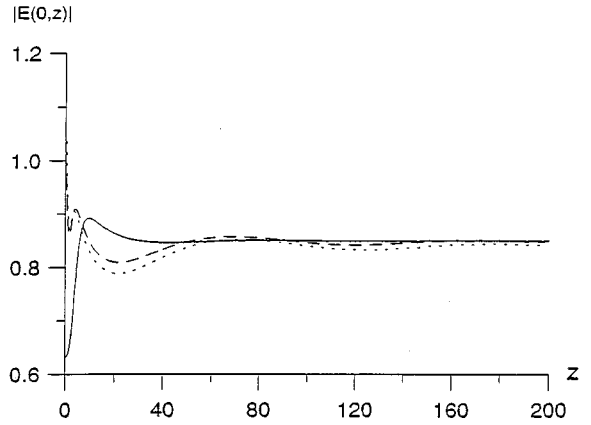

FIG. 9. Evolution of the pick amplitude of beams $|E(0,z)|$ as a function of the propagation distance z, for three different initial intensities (B, C, and D).

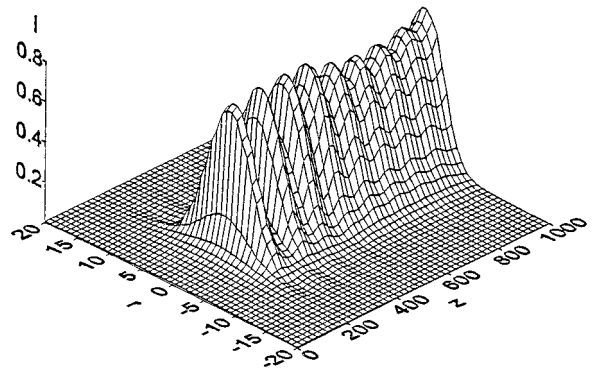

FIG. 10. Formation of pulsating light bullet for $N=150$ and for initial intensity $A_0^2=0.01$.

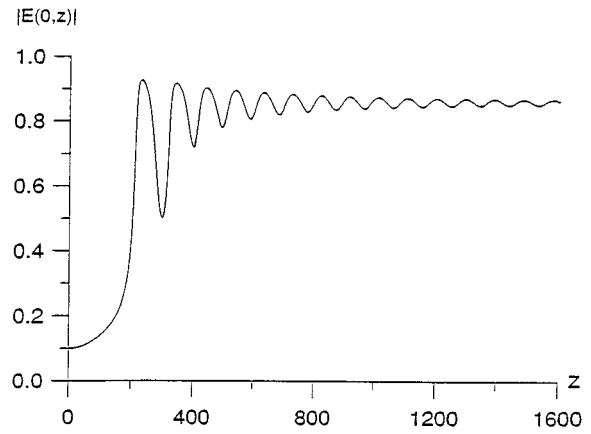

FIG. 11. Dynamics of the pick amplitude of beams $|E(0,z)|$ for $N=150$ and $A_0^2=0.01$.

lous group velocity dispersion is assumed to be $D=7\times10^{-26}\ \mathrm{s}^2/\mathrm{cm}$ [2]. Although this value may be far from the real one, it will not greatly affect the rough estimations of light bullets parameters, used with the purpose to illustrate quantitatively light bullets generation.

Equations (1) and (2) are converted in dimensionless Eq. (3) with nonlinearity (22) using the following normalizations: t/T, z/Z, $r_\perp/R$, and I/I_0, where $T=(\lambda D/4\pi n_2 I_0)^{1/2}=3.43$ fs, $R=\lambda/(8\pi^2 n_0 n_2 I_0)^{1/2}=0.48$ μm and $Z=\lambda/(2\pi n_2 I_0)=33.7$ μm. I_0 is the intensity of EM field for which the nonlinear refraction index becomes zero, $I_0=n_2/|n_4|=2.75\ \mathrm{GW/cm}^2$. The value used for the linear index is $n_0=1.88$ [8]. The pulse energy is given by the expression $W=[(\pi)^{3/2}/4]I_0R^2TN$, where N is dimensionless energy [see Eq. (13)]. Therefore, the numerically obtained critical self-trapping energy $N_c=34.04$ corresponds in dimensional units to $W_c=1.35$ pJ. Above this critical energy it is possible to create light bullets with intensity I satisfying the condition $0.41I_0<I<0.91I_0$, i.e., $1.38\ \mathrm{GW/cm}^2<I<2.5\ \mathrm{GW/cm}^2$ (see Fig. 3). The spatial transverse radius ρ and temporal width t_L corresponding to the longitudinal size of such a light bullet near the critical energy are, respectively, $\rho_c=2$ μm and $t_{Lc}=15$ fs, thus they are close to the diffraction and dispersion limits and consequently difficult to realize experimentally. Notice the interdependence of spatial radius and temporal width $\rho/R=t_L/T=a$. Therefore, in order to realize in practice the light bullets the beam energy has to be several times larger than the critical one. However, following requirements for producing all-optical logical systems, it is highly desirable to generate light bullets with small input laser intensities. The demonstrated robustness of light bullets allows us to choose the initial intensity much lower than the equilibrium one (region I in Fig. 3). For instance, for a pulse with energy $W=6$ pJ corresponding to dimensionless energy $N=150$, the minimum value of dimensionless initial intensity is $A_0^2=0.01$ (see Fig. 10). This input intensity corresponds in real units to $I_{\mathrm{inp}}=28\ \mathrm{MW/cm}^2$ for $\rho_{\mathrm{imp}}=11.86$ μm and $t_{L\mathrm{imp}}=84.5$ fs. Further evolution, following our analytical and numerical predictions, will be toward the stable equilibrium around which the light bullet will exhibit damped pulsations (see Fig. 10 and especially Fig. 11 where the dumping is more obvious). Notice that although the initial beam radius is larger than the critical one (ρ_c) the beam breaking (filamentation) does not occur. Corresponding equilibrium intensity, radius, and temporal width are, respectively, $I_e=2.36\ \mathrm{GW/cm}^2$, $\rho_e=2.8$ μm, and $t_{Le}=20$ fs. In practice the energy can be much higher, allowing even lower input intensity. Notice that nearly coinciding numerical and analytical equilibrium curves in Fig. 3 approach asymptotically the same minimum intensity value. Therefore, the hypothetical inverted PTS or some similar new material satisfying the low power requirement may potentially be used as the medium for all-optical logic devices.

We would like to emphasize that the results obtained in this paper can be applied not only to some hypothetical inverted PTS but also to many other media such as gaseous plasma, as well as semiconductor plasma. In unmagnetized plasmas the group velocity dispersion is anomalous. In gaseous plasmas saturating nonlinearities frequently appear due to the plasma density variation induced by high frequency pressure as well as due to the relativistic electron mass variation in the strong EM field [11]. In narrow gap semiconductors nonparabolicity of the electronic conduction band induces the nonlinearity related to conduction electrons [16]. Combined effects of this nonlinearity and the nonlinearity caused by two-photon generation of nonequilibrium free carriers, provided that the duration of light pulses exceeds their lifetime, give rise to the examined nonlinearity corresponding to Eq. (22) [17].

We demonstrated using the variational approach under which conditions the light beam is self-guided, generating light bullets in (3+1) dimensions. The main result obtained using the established analytical formalism is to elucidate the mechanism of how the light bullets, as completely localized structures, appear even if parameters of the initial beam are far from equilibrium. As a consequence, the choice of parameters for which the stable spatiotemporal solitons are created and persist is relatively large; i.e., it is not restricted to a domain near the equilibrium solution. Therefore, the light bullets are robust objects. The numerical simulations not only confirm predictions of the analytical approach but also demonstrate even stronger robustness of bullets that can appear in a considerably enlarged range of parameters. The

light-bullet generation is numerically demonstrated even for some initial amplitudes lying out of domains I and II in Fig. 3, due to the simultaneous creation of radiation spectrum (see Fig. 8). Thus, only one part of the beam is self-guided since the superfluous residue is radiated out. Due to their complete localization, robustness, and low energy, light bullets appear to be the best candidate for carrying the information that has to be treated in all-optical logic circuits.

[1] H. A. Haus and W. S. Wong, Rev. Mod. Phys. **68**, 423 (1996).
[2] R. McLeod, K. Wagner, and S. Blair, Phys. Rev. A **52**, 3254 (1995).
[3] Y. Silberberg, Opt. Lett. **15**, 1282 (1990); K. Hayata and M. Koshiba, *ibid.* **17**, 841 (1992); N. Akhmediev and J. M. Soto-Crespo, Phys. Rev. A **47**, 1358 (1993); D. E. Edmundson and R. H. Enns, *ibid.* **51**, 2491 (1995).
[4] A. C. Newell and J. V. Moloney, *Nonlinear Optics* (Addison-Wesley, New York, 1992).
[5] V. E. Zakharov and A. B. Shabat, Zh. Eksp. Teor. Fiz. **61**, 118 (1971) [Sov. Phys. JETP **34**, 62 (1972)].
[6] N. G. Vakhitov and A. A. Kolokolov, Izv. Vyssh. Uchebn. Zaved. Radiofiz. **16**, 1020 (1973) [Sov. Radiophys. **9**, 262 (1973)]; J. Juul Rasmussen and K. Rypdal, Phys. Scr. **33**, 481 (1986).
[7] B. L. Lawrence *et al.*, Phys. Rev. Lett. **73**, 597 (1994); B. L. Lawrence *et al.*, Electron. Lett. **30**, 447 (1994); B. L. Lawrence, *et al.*, Appl. Phys. Lett. **64**, 2773 (1994).
[8] E. M. Wright, B. L. Lawrence, W. Torruellas, and G. Stegeman, Opt. Lett. **20**, 2481 (1995).
[9] S. A. Akhmanov, A. P. Sukharukov, and R. V. Khokhlov, Usp. Fiz. Nauk **93**, 19 (1967) [Sov. Phys. Usp. **10**, 609 (1968)].
[10] J. F. Lam, B. Lippman, and F. Tappert, Phys. Fluids **20**, 1176 (1977).
[11] D. Anderson and M. Bonnedal, Phys. Fluids **22**, 105 (1979); D. Anderson, Phys. Rev. A **27**, 3135 (1983); M. Karlsson, *ibid.* **46**, 2726 (1992); V. I. Berezhiani and S. M. Mahajan, Phys. Rev. E **52**, 1968 (1995).
[12] V. E. Zakharov, V. V. Sobolev, and V. C. Synakh, Zh. Eksp. Teor. Fiz. **60**, 136 (1971) [Sov. Phys. JETP **33**, 77 (1971)].
[13] J. H. Marburger, Prog. Quantum Electron. **4**, 35 (1975); V. E. Zakharov and V. C. Synakh, Zh. Eksp. Teor. Fiz. **68**, 940 (1975) [Sov. Phys. JETP **41**, 465 (1976)].
[14] W. Torruellas, B. L. Lawrence, and G. Stegeman, Electron. Lett. **32**, 2092 (1996).
[15] G. G. Luther *et al.*, Opt. Lett. **19**, 862 (1994); L. Berge *et al.*, J. Opt. Soc. Am. B **13**, 1879 (1996).
[16] V. I. Berezhiani and S. M. Mahajan, Phys. Rev. Lett. **73**, 1840 (1994).
[17] A. A. Borshch, M. Brodin, and V. Volkov, *International Handbook: Laser Science and Technology* (Harwood Academic Publishers, Chur, 1990); V.I. Berezhiani and V. Skarka (unpublished).